

Interferometric Phase Shift Technique for High Resolution Deep UV Microlithography

Frank K. Tittel, Joseph R. Cavallaro, Motoi Kido*, Michael C. Smayling**, Gabor Szabó***, and William L. Wilson,

Department of Electrical and Computer Engineering, Rice University, P.O. Box 1892,
Houston, Texas 77251

* Nippon Steel Corporation, Kanawaga 229, Japan

** Texas Instruments Inc., Stafford, Texas 77477

*** Department of Optics and Quantum Electronics, Jate University, H-6720 Szeged, Hungary

ABSTRACT

A new phase shifting technique based on interferometry has been developed which is especially suited for deep-UV microlithography. Using only a single layer chromium mask, with no additional phase shift elements, significant resolution and contrast enhancement over conventional transmission lithography can be achieved. Both computer simulations, as well as experiments using a CCD camera and UV photoresist confirm the capabilities of this new approach. Using a relatively simple experimental setup and an illumination wavelength of 355 nm, lines with feature sizes as fine as 0.3 μm were achieved.

KEYWORDS: Phase shift, microlithography, excimer laser.

1. INTRODUCTION

Future high density integrated circuit designs will require advanced photolithographic techniques. Phase shifting is considered one of the most promising techniques for achieving higher resolution^{1,2,3}. In recent years, many phase shifting methods have been proposed to achieve smaller feature size and higher contrast for photolithographic images. These techniques, however, have several limitations. It has been difficult to build the necessary phase shifting elements into the photolithographic mask. Defects are hard to identify, and repair is also quite difficult if not impossible to achieve. As a result, mask yields are at present quite low and their cost is high. These limitations have slowed the introduction of phase shifting into the production line of high density DRAMs. Furthermore, the need to introduce deep UV illumination from excimer lasers makes the task of finding suitable transparent optics (masks and lenses) considerably more difficult.

A new approach to phase shifting has been developed⁴ that does not require any special "optically thick" phase shifting elements to be incorporated into the mask. It is based on a conventional single-layer chrome mask used in a unique interferometric arrangement. The approach is shown in Fig. 1. The single-layer chrome reticle is used as both a reflective and a transmissive element. An incoming laser beam is divided by a beam splitter. These beams illuminate the mask from both the front and back side via an additional beam splitter and mirror as shown. The reflected and transmitted beams are then colinearly combined and focused onto the substrate. The optical paths of the beams are chosen so that the phase of the two beams differs by an odd multiple of π radians when they are projected onto the surface of the substrate. This is accomplished by carefully adjusting the position of the mask to achieve the desired phase shift between the transmitted and reflected beams. As is demonstrated in Figure 2, the two out-of-phase beams cancel each other when they overlap, resulting in higher resolution than is possible with conventional photolithography.

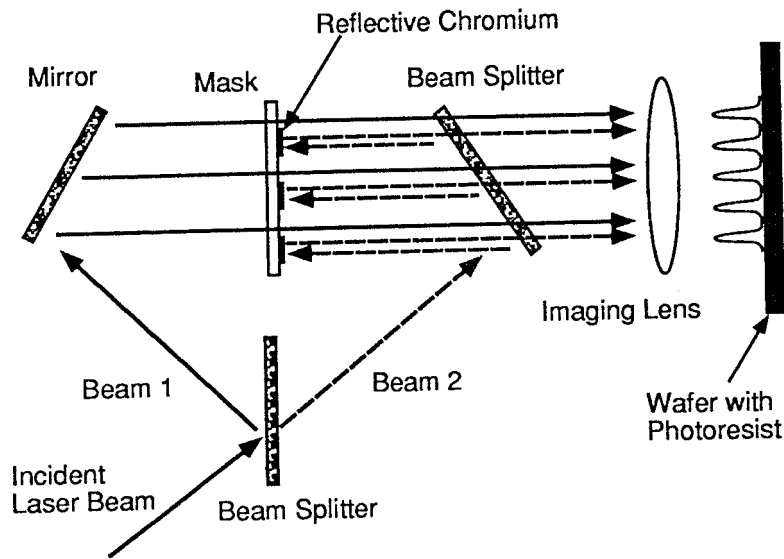


Figure 1 - New phase shifting scheme.

It is important that the difference in their overall length is less than the coherence length of the illumination source, in order to achieve the desired interferometric effect. This is an essential difference between this new method and more conventional phase shifting approaches. The net result of this technique is very much like that which is achieved by the chromeless phase-shifting.⁵ The essential difference is that a conventional chrome mask is used instead of the more difficult to fabricate, multi-layer dielectric mask. As mentioned above, this new phase shifting method will be particularly useful for short wavelengths, such as KrF illumination at 248 nm⁶, where it becomes increasingly difficult to find appropriate materials with which to fabricate the phase shifting elements.

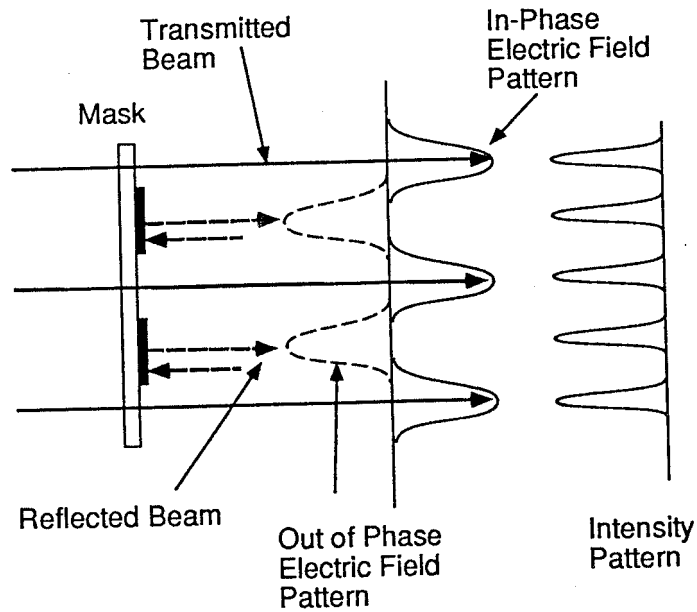


Figure 2.- Phase shifting effect obtained by interferometry.

2. SIMULATIONS

The new phase shift approach was compared with more conventional phase shift techniques using the DEPICT⁷ photolithography simulator. Alternating clear and opaque lines were used to model the normal transmission approach. A 180° phase shift in alternate clear regions was added to model the more conventional phase shifting approach. In order to simulate the new method, only clear regions were used, with a 180° phase shift inserted for each neighboring line. The lines with 0° phase shift were used to model the transmitting regions of the mask, while the lines with 180° phase shift corresponded to the reflecting regions of the mask. The imaging lens was assumed to have a numerical aperture of 0.4. Because illumination from a laser with a stable mode resonator was being modeled, a spatial coherence (σ) of 0.05 was assumed.

The minimum image resolution, W , can be expressed as

$$W = K_1 \frac{\lambda}{NA} \quad (1)$$

where λ is the irradiating laser wavelength, NA is the numerical aperture⁸ of the imaging lens. K_1 is an empirical parameter ~ 0.5 which takes into account non-ideal limitations in the system being considered. In order to make relative comparisons for the different photolithographic techniques, we introduce a new variable κ , which corresponds to the K_1 in equation (1) but which is now a function of the minimum feature size W as well as λ and NA .

$$\kappa(W, \lambda, NA) = \frac{W \cdot NA}{\lambda} \quad (2)$$

A comparison of κ for different photolithographic methods, removes system specific effects such as wavelength or numerical aperture.

The contrast C , of the final image is defined as

$$C = \frac{I_{\text{peak}} - I_{\text{min}}}{I_{\text{peak}} + I_{\text{min}}} \quad (3)$$

Here I_{peak} is the intensity at pattern maximum and I_{min} is the intensity at its minimum. For images formed by phase shifting technique, DEPICT simulations show that I_{min} remains nearly zero, while I_{peak} decreases as the feature size is reduced. In an image formed from two out-of-phase adjacent lines, there is always a location where the two overlapping images just cancel each other out, making $I_{\text{min}} = 0$. With $I_{\text{min}} = 0$, the contrast is nearly 100%, even though the quality of the resultant pattern, due to more overlap of out-of-phase images, is seriously degraded. In order to take this effect into account when evaluating different photolithographic techniques, we introduce a performance index (PI)

$$PI = I_{\text{peak}} C = I_{\text{peak}} \frac{I_{\text{peak}} - I_{\text{min}}}{I_{\text{peak}} + I_{\text{min}}} \quad (4)$$

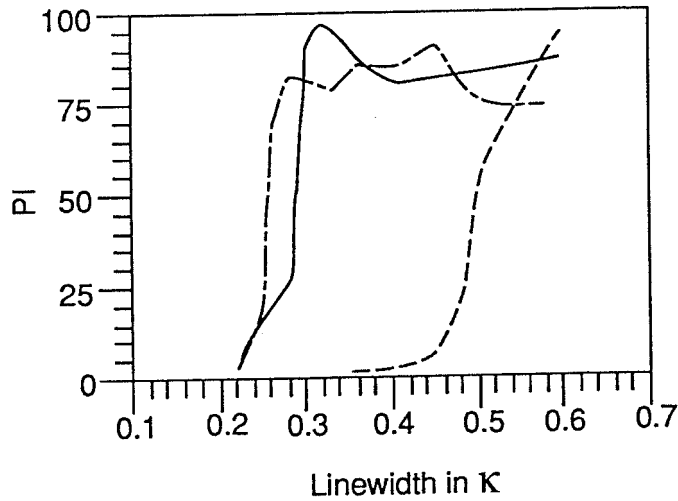


Figure 3. Results of Depict Simulation. The dashed line is for a conventional mask, the solid for Levinson-type phase shifting and the dot-dash for the new approach.

Figure 3 shows the results of DEPICT simulations of three photolithographic techniques, where the performance index PI is plotted as a function of K or normalized line size. Both phase shift approaches show significant advantages over the conventional transmission mask performance.

As can be seen, the performance index of the transmission mask decreases rapidly for K less than about 0.5, which agrees well with equation 2. The performance index for either phase shifting approach remains high for K down to about 0.26. This corresponds to a minimum feature size of about 0.2 μm for KrF (248 nm) illumination. Hence, this new phase shifting technique could potentially provide the 0.25 μm technology that would be required for the fabrication of a 256 Mbit DRAM.

Alignment and path-length errors can also have an impact on system performance. Alignment errors caused by the position of the imaging lens and the silicon wafer are exactly the same as in conventional phase shifting and transmission mask approaches. A mask positioning error that determines the difference of the optical paths between the two beams and a superposition error caused by misalignment of the two separate images are new parameters special to this method. The alignment parameters of the new phase shifting method are adjustable.

Several of these possible errors were studied using DEPICT and a two dimensional ray-tracing program. The phase error (PE) is defined as

$$PE = 180^\circ - |\phi_1 - \phi_2|. \quad (5)$$

Here, ϕ_1 is the phase of the transmitted beam and ϕ_2 is the phase of the reflected beam. The attenuation error (AE) is defined as the intensity ratio between the transmitted and the reflected beam

$$AE = \frac{I_{\text{trans}}}{I_{\text{ref}}}. \quad (6)$$

The superposition error (SE) is defined by the offset of the peak position of the transmitted image from its desired position.

$$SE = \frac{S}{(L/2)}, \quad (7)$$

Here L is the period of the transmitted image on the mask, and S is the offset distance of the image. Since the reflected and transmitted beams may not be parallel, this can cause a superposition error in the resulting image. This error is difficult to analyze using the DEPICT simulator, since it considers only a single directional light source. In order to analyze this somewhat unique alignment error, a two dimensional ray-tracing program was developed which calculates the one dimensional intensity distribution of the illuminating beams on the substrate surface image. With this program, it was possible to simulate the effect of superposition error for various optical parameters, such as different values of NA or defocusing conditions.

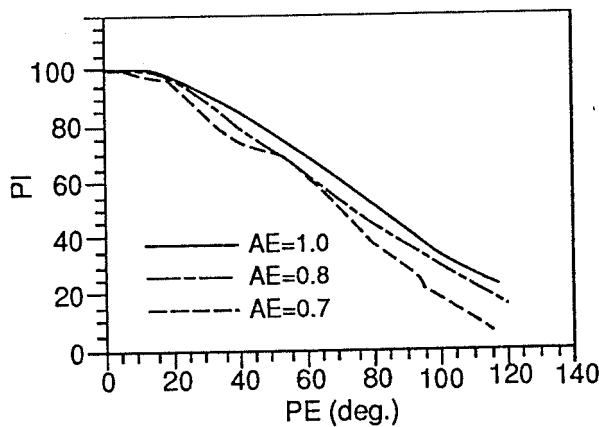


Figure 4. - Effect of phase and alignment errors

Figure 4 shows how the performance index changes with increasing phase error for various attenuation errors. If we define the maximum error tolerance as the phase error that reduces the contrast to 60 % (the approximate minimum requirement to produce a usable photoresist feature.), then the maximum error tolerance is approximately 60 degrees. This corresponds to a mask position error of 118 nm for 355 nm 3rd harmonic Nd:YAG. An attenuation error of 20 % degrades the image contrast by only about 10 %, and is obviously not a significant effect.

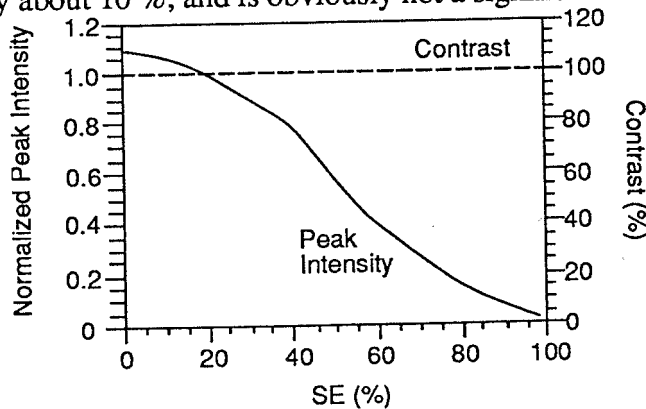


Figure 5. - Effect of superposition error on contrast and intensity.

Figure 5 shows the results of misalignment due to non-parallel image beams. It indicates that while the superposition error does not reduce contrast (it remains nearly 100 % over the entire range), the peak intensity steadily decreases with increasing superposition error. Thus, the superposition error significantly reduces the performance index and can significantly increase the required exposure time. The superposition error can easily be held to less than 10 % with a system that monitors the focused image, and thus the most important parameter that must be controlled is the phase error.

3. EXPERIMENTS AND DISCUSSION

A series of experiments were carried out in order to evaluate the feasibility and performance of this new approach to phase shifting. A CCD camera was used to quantify the intensity distribution pattern generated by the new method. Additionally, patterns were written onto Hoechst Celanese AZ1350B-SF photoresist with both a continuous (CW) and a pulsed laser source. A 100 mW Ar⁺ laser (457 nm, TEM₀₀ mode, 1.4 mm beam diameter) was used initially. A Nd:YAG laser (operated at 355 nm using third harmonic generation, 2.0 mJ, with a pulse duration of 10 ns and a repetition rate of 10 PPS) was used to investigate pulsed UV illumination. The experimental setup is shown in Fig. 6. A 20X microscope objective lens with a 0.4 NA was used as the imaging lens for the visible laser experiments. A 20X objective with UV transmitting glass and a 0.5 NA was used for the UV laser illumination experiments. The mask was a single layer of chromium with a number of different line and space patterns. The line sizes of the patterns varied from 2 to 22 μm. Optical evaluation of the resulting patterns were performed with a CCD camera system with a 0.8 NA and a magnifier that expanded the focused image onto the CCD image plane. Each CCD pixel corresponded to about 0.01 μm in the focused image plane. Beam profiling software was used to analyze the intensity distribution at the image plane.

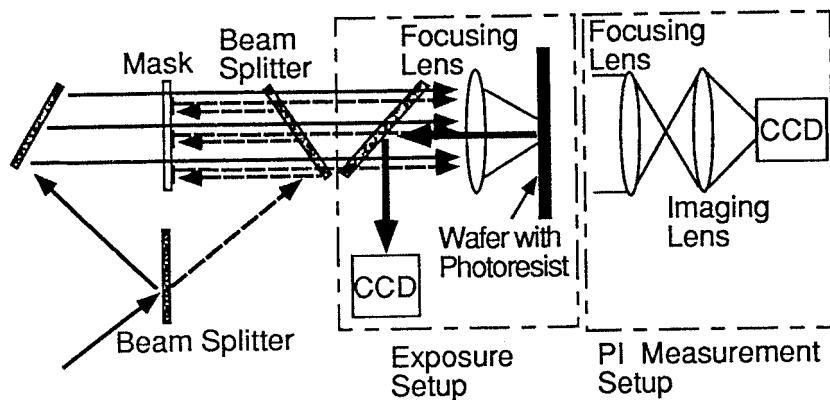


Figure 6.- Experimental arrangement

Patterns were also written on AZ1350B-SF UV photoresist. During photoresist exposure, the CCD camera was used to observe the reflected image from the silicon wafer in order to aid in alignment.

Figure 7 shows how the performance index varied for different line sizes. At 632 nm, the experimental data and the DEPICT simulation agree well. In both the experiment as well as the simulation, line widths corresponding to a K of slightly less than 0.27 (corresponding to a feature

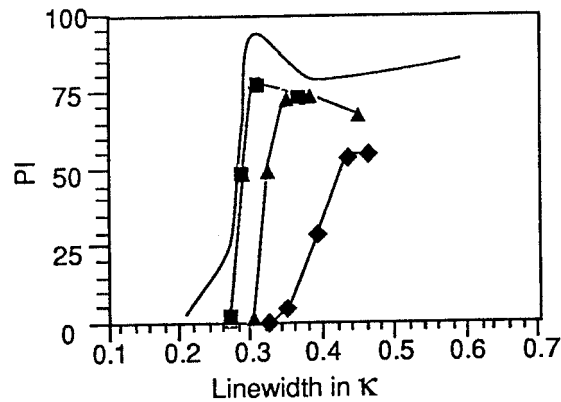


Figure 7.- A comparison of performance index (PI) obtained from simulation and experiment. The solid curve is the simulation shown in Fig 3. The square and triangle data are for CW exposures at 632 and 457 nm. The diamond represent the pulsed UV experiments at 355 nm.

size of about 0.66λ) were achievable. At 457 nm, the experimental results showed slightly reduced resolution, with a minimum K of about 0.3 (corresponding to a 0.75λ feature size). However, for pulsed 355 nm UV experiments using the third harmonic of a wide bandwidth (~ 30 GHz) Nd:YAG laser, the performance index is reduced corresponding to a minimum K of about 0.4 (feature size of 0.8λ).

Experiments were conducted using the UV photoresist at both 457 nm and 355 nm. A layer of photoresist approximately $0.5 \mu\text{m}$ thick was deposited on a 1.5 inch diameter silicon wafer by spinning the wafer at 3000 rpm. A laser beam intensity density of $50 \text{ mW}/\text{cm}^2$ at 457 nm was used to expose the wafer for 4 seconds, resulting in a deposited energy density of $200 \text{ mJ}/\text{cm}^2$ in the photoresist. This produced a $0.57 \mu\text{m}$ wide line pattern in the resist. The frequency tripled Nd:YAG exposure at 355 nm consisted of a train of 5 pulses, with a pulse duration of 10 ns, having a total deposited energy density of $30 \text{ mJ}/\text{cm}^2$. Figure 8 is a SEM photograph of the features obtained using UV laser illumination. A line size of $\leq 0.30 \mu\text{m}$ was obtained, which demonstrates the important practical capability of this new phase shifting method.

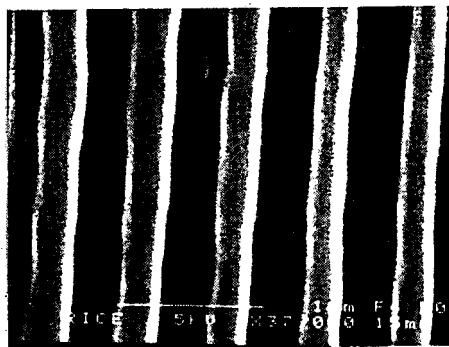


Figure 8. SEM Photo of $0.3 \mu\text{m}$ lines written in photoresist